Available online at www.sciencedirect.com
SCIENCE DIRECT®
Journal of Molecular Catalysis A: Chemical 224 (2004) 133–144
JOURNAL OF MOLECULAR CATALYSIS A: CHEMICAL
www.elsevier.com/locate/molcata

A study of *syn–anti* isomerism of six-coordinate ruthenium(II) complexes containing $PhP(CH_2CH_2CH_2PCy_2)_2$ (Cyttp) ligand☆

Patrick W. Blosser, Judith C. Gallucci[1], Andrew Wojcicki*

Department of Chemistry, The Ohio State University, 100 W. 18th Avenue, Columbus, OH 43210-1185, USA

Received 5 April 2004; received in revised form 22 July 2004; accepted 26 July 2004

Dedicated to Professor Józef J. Ziółkowski on the occasion of his 70th birthday.

Abstract

A study is reported on synthesis and ligand substitution/modification reactions of the *syn* and *anti* geometric isomers of the six-coordinate ruthenium(II) complexes [*mer*-Ru(κ^2-O_2CX)(CO)(Cyttp)]^n ($n=0$, X = O (**2**); $n=+1$, X = Me (**3**), Ph (**4**), OMe (**5**), OEt (**6**); Cyttp = $PhP(CH_2CH_2CH_2PCy_2)_2$) and *cis-mer*-RuX_2(CO)(Cyttp) (X = I (**7**), Cl (**8**)) (*syn* (**s**) and *anti* (**a**) refer to the orientation of the Ph group on the central P atom of Cyttp). Reaction of *cis-mer*-Ru$(BF_4)_2$(CO)(Cyttp) (**1**) in freshly prepared aqueous acetone solution with each of sodium carbonate, sodium acetate, and sodium benzoate affords **2a**, **3a**(BF_4), and **4a**(BF_4), respectively. The *syn* isomer of **2a**, **2s**, was synthesized by prolonged treatment of solid *mer*-Ru$(CO)_2$(Cyttp) with gaseous O_2. Complexes **2a** and **2s** do not interconvert even on heating in toluene or methanol at reflux temperature for 24 h. Alkylation of **2a** and **2s** with 1 equiv. of $[Me_3O]BF_4$ or $[Et_3O]PF_6$ affords the methylcarbonato (**5a**(BF_4) and **5s**(BF_4), respectively) and ethylcarbonato (**6a**(PF_6) and **6s**(PF_6), respectively) complexes. Use of >2 equiv. of $[Me_3O]BF_4$ still furnishes **5s**(BF_4) from **2s**, but yields **1** instead of **5a**(BF_4) from **2a**. The foregoing reactions represent, to our knowledge, the first example of different reactivity of *syn* and *anti* isomers of metal Cyttp complexes. Prolonged treatment of **2a** with an excess of MeI at room temperature results in the formation of **7a**. A parallel reaction of **2s** with MeI to yield **7s** requires heating; at ambient temperature, **5s**(I) is obtained instead. Each of the complexes **2**, **3**(BF_4)–**5**(BF_4), and **6**(PF_6) is converted to **8** with retention of the *syn* or *anti* configuration by the action of hydrochloric acid. It is concluded from this and previous studies that complexes stable to ligand dissociation do not undergo *syn–anti* isomerization, in contrast to those that contain weakly coordinated ligands. $^{13}C\{^1H\}$ and $^{31}P\{^1H\}$ NMR spectroscopic generalizations were developed that enable *syn–anti* assignment to be made for this class of complexes. The structures of **2a** (as **2a**·CH_2Cl_2·$2H_2O$), **2s** (as **2s**·(3/4)MeC(O)Me·$2H_2O$), and **5s** (as **5s**(BF_4)·C_6H_6) were determined by single crystal X-ray diffraction analysis.

Keywords: Ruthenium complexes; Triphosphine complexes; Carbonato complexes; *syn–anti* isomerism; Ligand substitution; Crystal structures

1. Introduction

Transition-metal complexes with polydentate phosphine ligands have attracted considerable attention in the past few decades largely because of their diverse structures and catalytic properties [1,2]. Such ligands provide an important advantage over monodentate phosphine ligands with respect to greater control of the coordination number, stoichiometry, and stereochemistry of their complexes.

Linear polydentate phosphines of the type $R_2P((CH_2)_nP)_m(CH_2)_nPR_2$ have been extensively utilized in

☆ Crystallographic data for the structural analysis have been deposited with the Cambridge Crystallographic Data Centre, CCDC nos. 228319, 227599, and 227406 for compounds **2a**·CH_2Cl_2·$2H_2O$, **2s**·(3/4)MeC(O)Me·$2H_2O$, and **5s**(BF_4)·C_6H_6, respectively. Copies of the data can be obtained free of charge from The Director, CCDC, 12 Union Road, Cambridge CB2 1EZ, UK (Fax: +44-1223-336-033; e-mail: mailto:deposit@ccdc.cam.ac.uk or http://www.ccdc.cam.ac.uk/).

* Corresponding author. Tel.: +1 614 292 4750; fax: +1 614 292 1685.
E-mail addresses: gallucci.1@osu.edu (J.C. Gallucci), wojcicki@chemistry.ohio-state.edu (A. Wojcicki).
[1] To whom inquiries concerning the X-ray crystallographic studies should be addressed. Fax: +1 614 292 1685.

1381-1169/$ – see front matter © 2004 Elsevier B.V. All rights reserved.
doi:10.1016/j.molcata.2004.07.029

the above context [1,3,4]. A representative member of this class, the tridentate $PhP(CH_2CH_2CH_2PCy_2)_2$ (Cyttp, Cy = *c*-C_6H_{11}), was prepared by Meek and coworkers [5], who also synthesized a number of its metal complexes and investigated their chemistry and possible catalytic applications [3]. Ruthenium complexes of Cyttp, e.g., $RuH_2(\eta^2\text{-}H_2)$(Cyttp) and RuHCl(Cyttp), show reactivities toward alkenes [6], alkynes [7,8], and CO_2-like species [9] that furnish information of relevance to catalytic processes. Later studies in our group resulted in the synthesis of $RuX_2(CO)$(Cyttp) (X = BF_4 or OSO_2CF_3) with two weakly coordinated anions; these complexes serve as useful precursors of a variety of ruthenium(II) complexes [10]. A rare example of a hydrido-oxo metal complex, $[ReH_2(O)(Cyttp)]^+$, which transfers both hydrogen and oxygen to some substrates and catalyzes hydration of nitriles to amides, was also reported [11,12].

Among the tridentate phosphines investigated, Cyttp shows exceptional propensity for meridional coordination around the metal. The trimethylene linkage between phosphorus atoms of Cyttp provides an ideal "chelate-bite" angle of ca. 90° for a larger transition metal such as ruthenium(II). As a result of this feature and of the steric demands of the terminal $-CH_2PCy_2$ donors, meridional structures are strongly favored. The consequence is greater control of the coordination geometry in metal complexes as compared to monodentate phosphine analogues.

In Cyttp complexes that are six-coordinate and contain different *trans* ligands (*cis* to all three P donors) as, for example, in *cis-mer*-ML_2L'(Cyttp), the Ph group on the central phosphorus atom can point to either one of them (L or L′), thus giving rise to *syn* and *anti* geometric isomers (cf. **I** and **II**).[2]

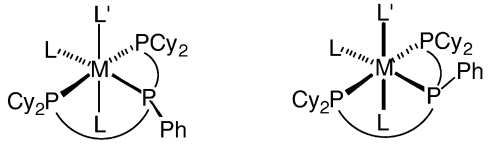

I **II**

Even when these *trans* ligands are identical, in some cases their inequivalence can be detected by NMR spectroscopy [12]. This type of *syn–anti* isomerism has been observed also for meridional ttp (ttp = $PhP(CH_2CH_2CH_2PPh_2)_2$) and related tridentate phosphine complexes [14,15]. Furthermore, it is not limited to phosphines. Particularly noteworthy are recent reports of synthesis and characterization of all possible geometric isomers of the amine complexes $[Co(dien)(ibn)Cl]^{2+}$ (dien = diethylenetriamine, ibn = 1,2-diamino-2-methylpropane) and $[Co(dien)(ampy)Cl]^{2+}$ (ampy = 2-aminomethylpyridine), including the meridional *syn* and *anti* species that result from different orientations of the NH hydrogen of dien [16,17].

There have been few studies on *syn–anti* isomerism of six-coordinate metal Cyttp complexes. Both isomers were synthesized for each of *cis-mer*-IrH_2Cl(Cyttp) [18,19],$[$*cis-mer*-$IrH_2(MeCN)(Cyttp)]^+$ [19], *cis-mer*-$RuH_2(P(OMe)_3)$(Cyttp) [20], *cis-mer*-$RuH_2(P(OPh)_3)$(Cyttp) [20], and *mer*-$RuCl(\eta^3\text{-}PhCH{=}C{-}C{\equiv}CPh)$(Cyttp) [7,8], some as a *syn–anti* mixture that was not separated. Characterization of at least one isomer in each case was effected by ^1H NMR nOe spectroscopy or X-ray diffraction techniques. Several other complexes of this general type were obtained as a single isomer and characterized similarly as *syn* or *anti* [8,10,19,20].

In this paper, we report further investigations into *syn–anti* isomerism of ruthenium(II) Cyttp complexes. In particular, we address questions concerning reactivity of such complexes in isomerization and ligand substitution/modification processes. Both *syn* and *anti* isomers of *mer*-$Ru(\kappa^2\text{-}O_2CO)(CO)$(Cyttp) (**2**) were synthesized and completely characterized, and their stereochemical behavior in the aforementioned types of transformation was investigated.

2. Experimental

2.1. General procedures and measurements

Reactions and manipulations of air-sensitive compounds were conducted under an atmosphere of dry argon by use of standard procedures [21]. Solvents were dried [22], distilled under argon, and degassed before use. Elemental analyses were carried out by M-H-W Laboratories, Phoenix, AZ. IR, NMR (^1H, ^{13}C, and ^{31}P), and mass spectra (FAB MS) were obtained as previously described [23,24]. All listed mass peaks are those of ions containing ^{102}Ru. Relative peak intensities are given with the assignments.

2.2. Materials

Reagents were procured from various commercial sources and used as received. The complexes *cis-mer-anti*-$RuI_2(CO)$(Cyttp) (**7a**), *cis-mer-anti*-$RuCl_2(CO)$(Cyttp) (**8a**), and *cis-mer*-$Ru(BF_4)_2(CO)$(Cyttp) (**1**) were prepared as reported earlier [10]. (Cyttp = $PhP(CH_2CH_2CH_2PCy_2)_2$; *mer* refers to Cyttp, and *cis* refers to I_2, Cl_2, etc.; the reference center for *syn* and *anti* is Ph on central P, cf. Section 1.)

2.3. Synthesis of carbonato, carboxylato, and alkylcarbonato complexes of Ru(CO)(Cyttp)

2.3.1. Preparation of *mer-syn*-$Ru(\kappa^2\text{-}O_2CO)(CO)$(Cyttp) (**2s**)

The procedure employed is a slight modification of that reported in the literature [25]. A powdery sample of known

[2] The designation *syn* and *anti* is made in accordance with the Cahn–Ingold–Prelog priority rules [13] as applied to the two ligands that are mutually *trans*.

[25] *mer*-$Ru(CO)_2$(Cyttp) (0.562 g, 0.755 mmol) in a Schlenk flask was exposed to a stream of O_2 gas for 10 days, during which time a gradual color change from pale yellow to slightly gray was observed. The solid was wetted with Et_2O (30 ml), collected on a filter frit, and washed with benzene (10 ml) to remove any remaining *mer*-$Ru(CO)_2$(Cyttp) and/or possible **2a** co-product. (*Note*: Whereas the solubility of **2s** in benzene is only ca. 0.025 g/10 ml, that of **2a** is greater than 0.25 g/10 ml.) Rinsing with Et_2O (20 ml) and drying under vacuum afforded **2s** as a white solid in 86% yield (0.506 g). Selected spectroscopic data. $^{13}C\{^1H\}$ NMR (CD_2Cl_2): δ (ppm) 205.2 (dt, $^2J_{PcC}$ = 17 Hz, $^2J_{PwC}$ = 12 Hz, CO), 166.6 (q, $^3J_{PC} \sim 1$ Hz, O_2CO), 35.1 (t, J_{PwC} = 11 Hz, CH of Cy), 34.0 (t, J_{PwC} = 9 Hz, CH of Cy). $^{13}P\{^1H\}$ NMR (CD_2Cl_2): δ (ppm) 22.5 (t, $^2J_{PcPw}$ = 30.5 Hz, P_c, 11.5 (d, $^2J_{PcPw}$ = 30.5 Hz, P_w). MS (FAB): *m/z* 777 (M^+, 14), 733 ($M^+ - CO_2$, 100).

2.3.2. Preparation of *mer-anti*-Ru(κ²-O_2CO)(CO)(Cyttp) (**2a**)

A solid mixture of *cis-mer*-$Ru(BF_4)_2$(CO)(Cyttp) (**1**) (0.428 g, 0.481 mmol) and Na_2CO_3 (0.065 g, 0.61 mmol) was dissolved in acetone (40 ml)/H_2O (25 ml), and the contents were stirred for 30 min. The volume of solution was reduced to ca. 20 ml to result in the formation of a white precipitate. The solid was collected on a filter frit, washed twice with 10-ml portions of H_2O and then with 10-ml portions of hexane, and dried under vacuum overnight. Yield of **2a**, 0.353 g (95%). IR (Nujol-hexachlorobutadiene): ν(CO) 1918 (vs), $\nu(O_2CO)$ 1668 (m), 1603 (s), 1235 (m) cm^{-1}. $^{13}C\{^1H\}$ NMR (CD_2Cl_2): δ (ppm) 209.0 (q, $^2J_{PcC} = {}^2J_{PwC}$ = 12 Hz, CO), 166.2 (s, O_2CO), 38.5 (t, J_{PwC} = 11 Hz, CH of Cy), 33.2 (t, J_{PwC} = 9 Hz, CH of Cy). $^{31}P\{^1H\}$ NMR (CD_2Cl_2): δ (ppm) 31.6 (t, J_{PcPw} = 31.9 Hz, Pc), 15.4 (d, J_{PcPw} = 31.9 Hz, P_w). MS (FAB): *m/z* 777 (M^+, 5), 733 ($M^+ - CO_2$, 100). Anal. Found: C, 58.71; H, 8.07%. Calc. for $C_{38}H_{61}O_4P_3Ru$: C, 58.82; H, 7.92%.

2.3.3. Preparation of [*mer-anti*-Ru(κ²-O_2CMe)(CO)(Cyttp)]BF_4 (**3a**(BF_4))

The product was obtained from *cis-mer*-$Ru(BF_4)_2$(CO)(Cyttp) (**1**) (0.200 g, 0.225 mmol) and sodium acetate (0.050 g, 0.61 mmol) by a procedure analogous to that for **2a** (Section 2.3.2). Yield of **3a**(BF_4), 0.161 g (83%). Selected spectroscopic data. IR (Nujol-hexachlorobutadiene): ν(CO) 1940 (vs), $\nu(O_2C)$ 1522 (m), 1455 (s), 1446 (s) cm^{-1}. ^1H NMR (CD_2Cl_2): δ (ppm) 2.03 (s, 3 H, Me). $^{13}C\{^1H\}$ NMR (CD_2Cl_2): δ (ppm) 206.6 (dt, $^2J_{PcC}$ = 15.6 Hz, $^2J_{PwC}$ = 11.5 Hz, CO), 187.1 (s, O_2C), 38.7 (t, J_{PwC} = 11.9 Hz, CH of Cy), 35.0 (t, J_{PwC} = 9.5 Hz, CH of Cy), 25.2 (s, Me). $^{31}P\{^1H\}$ NMR (CD_2Cl_2): δ (ppm) 40.0 (t, $^2J_{PcPw}$ = 30.4 Hz, P_c), 17.2 (d, $^2J_{PcPw}$ = 30.4 Hz, P_w). Anal. Found: C, 54.46; H, 7.27%. Calc. for $C_{39}H_{64}BF_4O_3P_3Ru$: C, 54.36; H, 7.49%.

2.3.4. Preparation of [*mer-anti*-Ru(κ²-O_2CPh)(CO)(Cyttp)]BF_4 (**4a**(BF_4))

The product was prepared from *cis-mer*-$Ru(BF_4)_2$(CO)(Cyttp) (**1**) (0.202 g, 0.227 mmol) and sodium benzoate (0.055 g, 0.38 mmol) by a procedure analogous to that for **3a**(BF_4). Yield of **4a**(BF_4), 0.180 g (86%). Selected spectroscopic data. IR (Nujol-hexachlorobutadiene): ν(CO) 1935 (vs), $\nu(O_2C)$ 1501 (m), 1495 (s), 1450 (s), 1435 (vs) cm^{-1}. $^{13}C\{^1H\}$ NMR (CD_2Cl_2): δ (ppm) 206.7 (dt, $^2J_{PcC}$ = 16 Hz, $^2J_{PwC}$ = 12 Hz, CO), 181.0 (q, $^3J_{PC}$ = 2 Hz, O_2C), 38.6 (t, J_{PwC} = 12 Hz, CH of Cy), 34.4 (t, J_{PwC} = 9.5 Hz, CH of Cy). $^{31}P\{^1H\}$ NMR (CD_2Cl_2): δ (ppm) 40.5 (t, $^2J_{PcPw}$ = 30.1 Hz, P_c), 17.3 (d, $^2J_{PcPw}$ = 30.1 Hz, P_w). Anal. Found: C, 57.24; H, 7.16%. Calc. for $C_{44}H_{66}BF_4O_3P_3Ru$: C, 57.21; H, 7.20%.

2.3.5. Preparation of [*mer-anti*-Ru(κ²-O_2COMe)(CO)(Cyttp)]BF_4 (**5a**(BF_4))

A stirred solution of *mer-anti*-Ru(κ²-O_2CO)(CO)(Cyttp) (**2a**) (0.140 g, 0.180 mmol) in 70 ml of CH_2Cl_2 was treated with $[Me_3O]BF_4$ (0.027 g, 0.182 mmol). After 1 h of stirring, the solvent was evaporated, and the ivory residue was washed consecutively with H_2O (20 ml) and hexane (30 ml) and dried overnight. Yield of **5a**(BF_4), 0.130 g (82%). Selected spectroscopic data. IR (Nujol-hexachlorobutadiene): ν(CO) 1940 (vs), $\nu(O_2CO)$ 1505 (m), 1450 (s), 1435 (sh), ν(COC) 1090 (s) cm^{-1}. ^1H NMR (CD_2Cl_2): δ (ppm) 3.84 (s, 3 H, OMe). $^{13}C\{^1H\}$ NMR (CD_2Cl_2): δ (ppm) 206.5 (dt, $^2J_{PcC}$ = 12 Hz, $^2J_{PwC}$ = 11 Hz, CO), 161.3 (s, O_2CO), 55.0 (s, OMe), 38.4 (t, J_{PwC} = 12 Hz, CH of Cy), 34.5 (t, J_{PwC} = 9 Hz, CH of Cy). $^{31}P\{^1H\}$ NMR (CD_2Cl_2): δ (ppm) 40.1 (t, $^2J_{PcPw}$ = 29.8 Hz, P_c), 15.9 (d, $^2J_{PcPw}$ = 29.8 Hz, P_w). MS (FAB): *m/z* 792 (M^+, 73), 718 ($M^+ + H - O_2COMe$, 100).

When this reaction was carried out with more than 2 equiv. of $[Me_3O]BF_4$, the only phosphorus-containing species detected in solution by $^{31}P\{^1H\}$ NMR spectroscopy was *cis-mer*-$Ru(BF_4)_2$(CO)(Cyttp) (**1**).

2.3.6. Preparation of [*mer-syn*-Ru(κ²-O_2COMe)(CO)(Cyttp)]BF_4 (**5s**(BF_4))

A procedure analogous to that in Section 2.3.5 was employed using $[Me_3O]BF_4$ (0.048 g, 0.324 mmol) and *mer-syn*-Ru(κ²-O_2CO)(CO)(Cyttp) (**2s**) (0.100 g, 0.129 mmol). Yield of **5s**(BF_4), 0.101 g (89%). Selected spectroscopic data. IR (Nujol-hexachlorobutadiene): ν(CO) 1960 (vs), $\nu(O_2CO)$ 1540 (m), 1490 (s), 1385 (s), ν(COC) 1088 (s) cm^{-1}. ^1H NMR (CD_2Cl_2): δ (ppm) 3.83 (s, 3 H, OMe). $^{13}C\{^1H\}$ NMR (CD_2Cl_2): δ (ppm) 203.1 (dt, $^2J_{PcC}$ = 21 Hz, $^2J_{PwC}$ = 11 Hz, CO), 161.3 (s, O_2CO), 55.0 (s, OMe), 36.1 (t, J_{PwC} = 11 Hz, CH of Cy), 34.5 (t, J_{PwC} = 10 Hz, CH of Cy). $^{31}P\{^1H\}$ NMR (CD_2Cl_2): δ (ppm) 30.9 (t, $^2J_{PcPw}$ = 28.5 Hz, P_c), 11.2 (d, $^2J_{PcPw}$ = 28.5 Hz, P_w). MS (FAB): *m/z* 791 ($M^+ - H$, 100), 717 ($M^+ - O_2COMe$, 97). Anal. Found: C, 56.07; H, 7.11%. Calc. for $C_{39}H_{64}BF_4O_4P_3Ru \cdot C_6H_6$: C, 56.55; H, 7.38%.

2.3.7. Preparation of [mer-anti-Ru(κ²-O_2COEt)(CO)(Cyttp)]PF_6 (**6a**(PF_6))

A procedure analogous to that in Section 2.3.5 was employed using [Et_3O]PF_6 (0.027 g, 0.109 mmol) and *mer-anti*-Ru(κ²-O_2CO)(CO)(Cyttp) (**2a**) (0.076 g, 0.098 mmol). Yield of **6a**(PF_6), 0.079 g (86%). Selected spectroscopic data: IR (Nujol-hexachlorobutadiene): ν(CO) 1950 (vs), ν(O_2CO) 1535 (m), 1482 (s), 1385 (m), ν(COC) 1075 (m) cm^{-1}. ^1H NMR ($CDCl_3$): δ (ppm) 4.27 (q, $^3J_{HH}$ = 7.1 Hz, 2 H, OCH_2), 1.35 (t, $^3J_{HH}$ = 7.1 Hz, 3 H, Me). $^{31}P\{^1H\}$ NMR ($CDCl_3$): δ (ppm) 39.8 (t, $^2J_{PcPw}$ = 30.3 Hz, P_c), 15.9 (d, $^2J_{PcPw}$ = 30.3 Hz, P_w). MS (FAB): *m/z* 805 ($M^+ - H$, 100), 717 ($M^+ - O_2COEt$, 72).

2.3.8. Preparation of [mer-syn-Ru(κ²-O_2COEt)(CO)(Cyttp)]PF_6 (**6s**(PF_6))

The title complex was prepared from *mer-syn*-Ru(κ²-O_2CO)(CO)(Cyttp) (**2s**) (0.110 g, 0.142 mmol) and [Et_3O]PF_6 (0.040 g, 0.161 mmol) by a procedure analogous to that in Section 2.3.5. Yield of **6s**(PF_6), 0.122 g (92%). Selected spectroscopic data. IR (Nujol-hexachlorobutadiene): ν(CO) 1950 (vs), ν(O_2CO) 1548 (s), 1490 (s), 1382 (m), ν(COC) 1080 (m) cm^{-1}. ^1H NMR ($CDCl_3$): δ (ppm) 4.25 (q, $^3J_{HH}$ = 7.1 Hz, 2 H, OCH_2), 1.37 (t, $^3J_{HH}$ = 7.1 Hz, 3 H, Me). $^{31}P\{^1H\}$ NMR ($CDCl_3$): δ (ppm) 30.7 (t, $^2J_{PcPw}$ = 28.4 Hz, P_c), 11.2 (d, $^2J_{PcPw}$ = 28.4 Hz, P_w). MS (FAB): *m/z* 805 ($M^+ - H$, 100), 717 ($M^+ - O_2COEt$, 11).

2.4. Reactions of carbonato complexes of Ru(CO)(Cyttp) with MeI

2.4.1. Preparation of cis-mer-anti-RuI_2(CO)(Cyttp) (**7a**)

Neat MeI (0.25 ml, 0.57 g, 4.0 mmol) was added to a stirred solution of *mer-anti*-Ru(κ²-O_2CO)(CO)(Cyttp) (**2a**) (0.105 g, 0.135 mmol) in 50 ml of benzene (and C_6D_6) at room temperature, and progress of reaction was monitored by $^{31}P\{^1H\}$ NMR spectroscopy. After a few minutes, new signals were observed at δ (ppm) 10.8 (t) and −0.9 (d) with $^2J_{PP}$ = 31.5 Hz. In the ^1H NMR spectrum (C_6D_6 solution), an additional resonance appeared at δ (ppm) 3.78 (s) and has been assigned to the same intermediate. With time, $^{31}P\{^1H\}$ resonances of **7a** [10] grew in, and those of the reaction intermediate decreased in intensity. After 48 h, solvent was removed under vacuum, and the residue was washed with hexane (10 ml). The bright yellow solid was filtered off and dried under vacuum. Yield of **7a**, 0.092 g (70%). Selected spectroscopic data. $^{13}C\{^1H\}$ NMR ($CDCl_3$): δ (ppm) 201.2 (q, $^2J_{PcC}$ = $^2J_{PwC}$ = 9 Hz, CO), 42.1 (t, J_{PwC} = 11 Hz, CH of Cy), 38.1 (t, J_{PwC} = 11 Hz, CH of Cy). $^{31}P\{^1H\}$ NMR ($CDCl_3$): δ (ppm) 7.8 (t, $^2J_{PcPw}$ = 30.5 Hz, P_c), −8.4 (t, $^2J_{PcPw}$ = 30.5 Hz, P_w).

2.4.2. Preparation of cis-mer-syn-RuI_2(CO)(Cyttp) (**7s**)

Neat MeI (0.25 ml, 0.57 g, 4.0 mmol) was added to a solution of *mer-syn*-Ru(κ²-O_2CO)(CO)(Cyttp) (**2s**) (0.100 g, 0.129 mmol) in 40 ml of THF, and the mixture was heated at reflux temperature for 10 h. The volatiles were then removed, hexane (20 ml) was added to the residue, and the yellow solid was filtered off and dried under vacuum. Yield of **7s**, 0.080 g (64%). Selected spectroscopic data. IR (Nujol): ν(CO) 1940 (vs) cm^{-1}. $^{13}C\{^1H\}$ NMR ($CDCl_3$): δ (ppm) 199.1 (dt, $^2J_{PcC}$ = 13 Hz, $^2J_{PwC}$ = 12 Hz, CO), 40.9 (t, J_{PwC} = 11 Hz, CH of Cy), 38.6 (t, J_{PwC} = 11 Hz, CH of Cy). $^{31}P\{^1H\}$ NMR ($CDCl_3$): δ (ppm) 5.4 (t, $^2J_{PcPw}$ = 27.2 Hz, P_c), −5.6 (t, $^2J_{PcPw}$ = 27.2 Hz, P_w). Anal. Found: C, 46.02; H, 6.44%. Calc. for $C_{37}H_{61}I_2OP_3Ru$: C, 45.83; H, 6.34%.

When this reaction was carried out in THF/toluene at room temperature for 16 h, the isolated product was [*mer-syn*-Ru(κ²-O_2COMe)(CO)(Cyttp)] I (**5s**(I)), as determined by ^1H and $^{31}P\{^1H\}$ NMR spectroscopy.

2.5. Reactions of carbonato, carboxylato, and alkylcarbonato complexes of Ru(CO)(Cyttp) with HCl

2.5.1. Preparation and characterization of cis-mer-syn-$RuCl_2$(CO)(Cyttp) (**8s**)

Concentrated hydrochloric acid (0.25 ml, ca. 3 mmol) was added to a stirred solution of *mer-syn*-Ru(κ²-O_2CO)(CO)(Cyttp) (**2s**) (0.270 g, 0.348 mmol) in 30 ml of CH_2Cl_2. Effervescence occurred immediately, and after 5 min the volume of solution was reduced to ca. 1 ml. Pentane (25 ml) was added with stirring, and the white solid was filtered off, washed with pentane (20 ml), and dried under vacuum overnight. Yield of **8s**, 0.160 g (58%). Selected spectroscopic data. IR (Nujol): ν(CO) 1930 (vs) cm^{-1}. $^{13}C\{^1H\}$ NMR (CD_2Cl_2): δ (ppm) 200.2 (dt, $^2J_{PcC}$ = 17 Hz, $^2J_{PwC}$ = 12 Hz, CO), 33.1 (t, J_{PwC} = 10 Hz, CH of Cy), 32.5 (t, J_{PwC} = 9 Hz, CH of Cy). $^{31}P\{^1H\}$ NMR (CD_2Cl_2): δ (ppm) 11.3 (t, $^2J_{PcPw}$ = 30.0 Hz, P_c), 4.6 (d, $^2J_{PcPw}$ = 30.0 Hz, P_w). Anal. Found: C, 56.27; H, 7.64; Cl, 8.89%. Calc. for $C_{37}H_{61}Cl_2OP_3Ru$: C, 56.48; H, 7.81; Cl, 9.01%.

2.5.2. Reactions of other Ru(CO)(Cyttp) complexes with HCl

In a typical reaction, *mer-anti*-Ru(κ²-O_2CO)(CO)(Cyttp) (**2a**) (0.020 g, 0.026 mmol) was dissolved in 0.5 ml of CH_2Cl_2 in a 5-mm NMR tube, and concentrated hydrochloric acid (0.05 ml, ca. 0.6 mmol) was added. After the tube was shaken for about 2 min, a $^{31}P\{^1H\}$ NMR spectrum was recorded. The only phosphorus-containing species detected was *cis-mer-anti*-$RuCl_2$(CO)(Cyttp) (**8a**) [10]. The same product was obtained by starting with each of [*mer-anti*-Ru(κ²-O_2CMe)(CO)(Cyttp)]BF_4 (**3a**(BF_4)), [*mer-anti*-Ru(κ²-O_2CPh)(CO)(Cyttp)]BF_4 (**4a**(BF_4)), [*mer-anti*-Ru(κ²-O_2COMe)(CO)(Cyttp)]BF_4 (**5a**(BF_4)), and [*mer-anti*-Ru(κ²-O_2COEt)(CO)(Cyttp)]PF_6 (**6a**(PF_6)). Similarly, reactions of concentrated hydrochloric acid with each of [*mer-syn*-Ru(κ²-O_2COMe)(CO)(Cyttp)]BF_4 (**5s**(BF_4)) and [*mer-syn*-Ru(κ²-O_2COEt)(CO)(Cyttp)]PF_6 (**6s**(PF_6)) afforded *cis-mer-syn*-$RuCl_2$(CO)(Cyttp) (**8s**).

2.6. Crystallographic analyses

All data were collected on a Rigaku AFC5S diffractometer at room temperature using Mo Kα radiation. Cell constants were determined by a least-squares fit of the diffractometer setting angles for 25 reflections in the 2θ range 20–30°. All calculations were done with the TEXSAN package [26]. Full matrix least-squares refinement was based on F. Hydrogen atoms are included in the models as fixed contributions in calculated positions with the assumption that C–H = 0.98 Å and $B(H) = B_{eq}(C)\cdot 1.2$. Scattering factors for neutral atoms and anomalous dispersion terms for non-hydrogen atoms were used [27]. A summary of the crystal data and the details of the intensity data collection and refinement are provided in Table 1.

2.6.1. Analysis of *mer-anti-Ru(κ²-O₂CO)(CO)(Cyttp)·CH₂C1₂·2H₂O* (**2a**·*CH₂Cl₂·2H₂O*)

The data collection crystal was a clear, colorless rod grown from a CH_2Cl_2/hexane solution. During data collection, six standard reflections were measured after every 150 reflections and indicated that a small amount of decomposition was occurring. The standards decreased in intensity by an average value of 6%. A linear decay correction was applied to the data. A series of ψ scans indicated that an absorption correction was unnecessary.

The asymmetric unit contains complex **2a**, a disordered molecule of CH_2Cl_2, and two H_2O molecules. The disordered CH_2Cl_2 was modeled by two orientations of the molecule with a common carbon atom. The site occupation factor for the primary orientation refined to a final value of 0.60(1). The disorder model was refined only isotropically. No hydrogen atoms were added to the CH_2Cl_2 molecule or to the two H_2O molecules. The top five peaks in the final difference electron density map range from 0.76 to 1.54 e $Å^{-3}$ and are all in the immediate vicinity of the disordered CH_2Cl_2 molecule.

2.6.2. Analysis of *mer-syn-Ru(κ²-O₂CO)(CO)(Cyttp)·(3/4)MeC(O)Me·2H₂O* (**2s**·*(3/4)MeC(O)Me·2H₂O*)

The data collection crystal was initially a clear, colorless chunk, which had been cut from a much larger crystal grown from an acetone/hexane layered solvent system. Six standard reflections were measured after every 150 reflections during data collection and exhibited a wide range of intensity variation. Two of the standards decreased in intensity by about 30%, while the decrease for the other four standards ranged from 8.5 to 13.6%. A linear decay correction was applied to the data based on the latter four standards. Upon visual inspection at the end of data collection, the crystal appeared cloudy and striated.

The structure suffers from much disorder. One of the trimethylene groups is disordered, with atom C(2) occupying two positions, labeled as C(2A) and C(2B). Atom C(2B) was refined only isotropically. The occupancy factor refined to 0.76(3) for C(2A), with C(2A) constrained at 0.24. There is a solvent molecule of acetone, which is refined with an occupancy factor of 0.75. There also appear to be three H_2O molecules in the asymmetric unit, and one of them is located on a twofold axis. The occupancy factors for all three H_2O molecules were refined and set at 0.79(3) for O(6) and 0.27(3) for O(8). The occupancy factor for the third H_2O oxygen, O(7), refined to a value of 1.02, and was fixed at 1.0 for the final cycles. Because of the large thermal parameters for the acetone and H_2O, these molecules were only refined isotropically, and no hydrogen atoms were added.

2.6.3. Analysis of *[mer-syn-Ru(κ²-O₂COMe)(CO)(Cyttp)]BF₄·C₆H₆* (**5s**(*BF₄*)·*C₆H₆*)

The data collection crystal, a clear, colorless rectangular rod, was cut from a larger crystal grown from a CH_2Cl_2/C_6H_6 solution. Six standard reflections were measured after every 150 reflections and indicated that a very small amount of crystal decomposition occurred during data collection. On the average, the intensities of the standards decreased by 1%, and the data were corrected for this small amount of decay. A correction for absorption was made by the empirical ψ scan method [28].

The asymmetric unit contains complex **5s**, a BF_4^- ion, and a benzene molecule of solvation. Several regions of this structure appear to be disordered. One of the trimethylene bridges, C(4)–C(5)–C(6), appears to have two positions for atom C(5). These are introduced into the model as atoms C(5A) and C(5B), with occupancy factors of 0.62 and 0.38, respectively, based on their peak heights from a difference electron density map. The BF_4^- ion is disordered, with two orientations for this group related by rotation about the B–F(1) bond. The B and F(1) atoms each have occupancy factors of 1.0; the occupancy factor for F(2A), F(3A), and F(4A) was refined to 0.71(1), and this then fixes the occupancy factor for F(2B), F(3B), and F(4B) (the second orientation) at 0.29. The BF_4^- ion was refined only isotropically. The benzene molecule of solvation appears to be disordered, since it acquires very anisotropic atomic displacement parameters. No attempt was made to model this disorder.

3. Results

3.1. Synthesis and reaction chemistry

The starting point of this investigation was synthesis of *syn* and *anti* isomers of *mer*-Ru(κ²-O_2CO)(CO)(Cyttp) (**2s** and **2a**, respectively). These preparative studies were then extended to the related carboxylato and alkylcarbonato complexes [*mer*-Ru(κ²-O_2CR)(CO)(Cyttp)]$^+$ (R = Me (**3**), Ph (**4**)) and [*mer*-Ru(κ²-O_2COR)(CO)(Cyttp)]$^+$ (R = Me (**5**), Et (**6**)), respectively. Carbonato, carboxylato, and alkylcarbonato ligand substitution reactions with chloride and iodide were also probed with respect to stereochemical changes.

Table 1
Summary of crystal data, data collection, and structure refinement parameters for **2a**·CH_2Cl_2·$2H_2O$, **2s**·(3/4)MeC(O)Me·$2H_2O$, and **5s**(BF_4)·C_6H_6

Compound	**2a**·CH_2Cl_2·$2H_2O$	**2s**·(3/4)MeC(O)Me·$2H_2O$	**5s**(BF_4)·C_6H_6
Empirical formula	$C_{38}H_{61}O_4P_3Ru·CH_2Cl_2·2H_2O$	$C_{38}H_{61}O_4P_3Ru·3/4C_3H_6O·2H_2O$	$C_{39}H_{64}BF_4O_4P_3Ru·C_6H_6$
Formula weight	896.85	856.46	955.84
Crystal system	Triclinic	Monoclinic	Monoclinic
Space group	*P*	*C*2/*c*	$P2_1/n$
a (Å)	14.231(3)	21.517(6)	14.464(2)
b (Å)	17.364(3)	18.714(3)	16.104(2)
c (Å)	9.230(2)	22.757(3)	20.822(2)
α (°)	93.10(2)		
β (°)	93.44(2)	101.85(1)	104.29(1)
γ (°)	104.83(2)		
V (Å^3)	2195.1(8)	8968(5)	4699.8(7)
Z	2	8	4
D_{calc} (g cm^{-3})	1.36	1.27	1.35
Crystal size (mm^3)	0.23 × 0.27 × 0.38	0.23 × 0.31 × 0.35	0.12 × 0.35 × 0.42
Linear abs. coeff. (cm^{-1})	6.20	4.88	4.80
2θ limits (°)	$4 \le 2\theta \le 55$	$4 \le 2\theta \le 50$	$4 \le 2\theta \le 55$
Data collected	$+h, \pm k, \pm l$	$+h, +k, \pm l$	$+h, +k, \pm l$
Scan type	$\omega - 2\theta$	ω	ω
No. of unique data	10066	8136	11170
No. of unique data with $F_o^2 > 3\sigma(F_o^2)$	6301	3335	5674
Final no. of variables	454	448	519
$R(F)$[a]	0.055	0.060	0.048
$R_w(F)$[b]	0.067	0.065	0.051
Error in observation of unit weight (e)	1.89	1.60	1.40
Maximum and minimum peaks in final map (e Å^{-3})	1.54, −0.91	0.77, −0.50	0.65, −0.81

[a] $R(F) = \sum ||F_o| - |F_c|| / \sum |F_o|$.
[b] $R_w(F) = [\sum w(|F_o| - |F_c|)^2 / \sum w|F_o|^2]^{1/2}$ with $w = 1/\sigma^2(F_o)$.

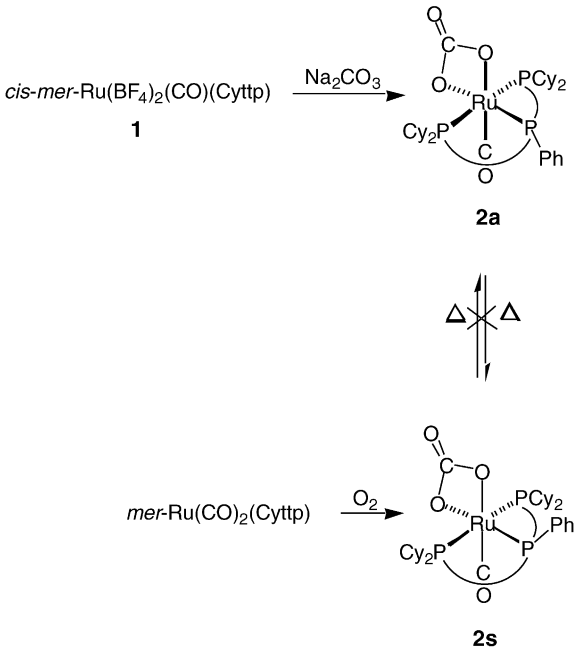

Scheme 1.

Complex *mer*-Ru(κ^2-O_2CO)(CO)(Cyttp) was reported by Meek et al. to be formed by reaction of the solid *mer*-$Ru(CO)_2$(Cyttp) with molecular oxygen [25] (Scheme 1) but was not characterized for the *syn* or *anti* configuration of its Cyttp phenyl group. By employing a slightly modified experimental procedure (cf. Section 2.3.1), we isolated pure **2s** as a white solid in very good yield. Its *syn* structure was established by X-ray diffraction techniques (vide infra). Attempts at isomerization of **2s** by heating in toluene or methanol at reflux for 24 h showed no evidence of such a transformation. The selective formation of **2s** upon oxidation of solid *mer*-$Ru(CO)_2$(Cyttp) by O_2 may be a result of the latter complex's crystal packing. It is possible that a molecule of O_2 can approach only one carbonyl ligand owing to Cyttp substituents protecting the other CO from attack leading to oxidation.

The *anti* isomer **2a** was synthesized by reaction of *cis-mer*-$Ru(BF_4)_2$(CO)(Cyttp) with Na_2CO_3 in acetone solution at room temperature (Scheme 1). Like **2s**, it also shows stability to *syn–anti* isomerization under comparable conditions. However, to obtain isomerically pure **2a** from **1** and Na_2CO_3, it is necessary to dissolve the reactants simultaneously (as a solid mixture) or to add solid **1** to Na_2CO_3 in solution. When a solution of **1** in acetone was stirred for 15 min and then treated with Na_2CO_3, both **2a** (ca. 85%) and **2s** (ca. 15%) were observed by $^{31}P\{^1H\}$ spectroscopy. The experiment shows that at the time of addition of Na_2CO_3, a mixture of **1a** and **1s** was present in solution. Solution behavior of **1**, as well as of the related *cis-mer*-$Ru(OSO_2CF_3)_2$(CO)(Cyttp), was investigated by variable-temperature $^{19}F\{^1H\}$ and $^{31}P\{^1H\}$ NMR spectroscopy [10]. Owing to the complexity of the spectra, which indicate a number of ongoing dynamic processes that most likely involve different coordination of the anionic ligands and their substitution by the solvent, the presence of *syn–anti* isomerization could not be inferred with complete

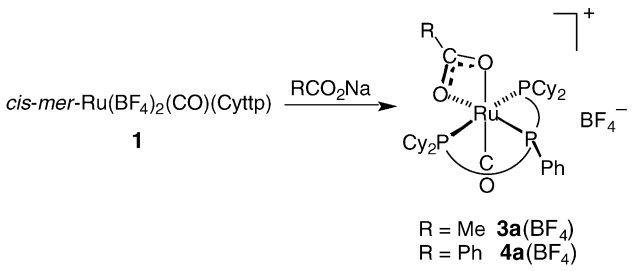

Scheme 2.

confidence. However, for the data to be consistent, such an isomerization would have to be relatively slow compared to the other occurring reactions.

The structure of **1** in the solid has not been elucidated; however, it is probably *anti*, like the structure of the related *cis-mer*-Ru(OSO_2CF_3)(CO)(Cyttp), established by X-ray diffraction techniques [10]. This is because both of these complexes were prepared by very similar reactions, viz., treatment of *cis-mer-syn*-RuH_2(CO)(Cyttp) (Cyttp Ph group *syn* to CO) with the appropriate acid, HBF_4 or CF_3SO_3H. Moreover, **1** and *cis-mer*-Ru(OSO_2CF_3)$_2$(CO)(Cyttp) undergo substitution of BF_4^- and $CF_3SO_3^-$ with other, stronger ligands, for example, H^- and I^-, in reactions that also proceed with retention of the orientation of the Cyttp Ph group toward the CO [10]. In contrast, use of the weaker ligands such as F^- and H_2O led to *syn–anti* isomerization; however, no rigorous order of addition of reactants was maintained in these substitutions.

The carboxylato complexes [*mer-anti*-Ru(κ^2-O_2CR)(CO)(Cyttp)]BF_4 (R = Me (**3a**(BF_4)), Ph (**4a**(BF_4))) were obtained by treatment of solutions of sodium acetate and benzoate, respectively, with **1** (Scheme 2). By following this order of introduction of reactants into solution, only a single *syn–anti* isomer was detected for each product by $^{31}P\{^1H\}$ NMR spectroscopy. Based on the considerations presented above, and from an analysis of the NMR data (cf. Section 3.2), both products are formulated as *anti*. No *anti* to *syn* isomerization was observed for **3a**(BF_4) and **4a**(BF_4).

The methylation reaction of **2a** with 1 equiv. of [Me_3O]BF_4 affords the methylcarbonato complex [*mer-anti*-Ru(κ^2-O_2COMe)(CO)(Cyttp)]BF_4 (**5a**(BF_4)) (Scheme 3). Surprisingly, when more than 2 equiv. of [Me_3O]BF_4 were employed, the only phosphorus-containing species detected in solution by $^{31}P\{^1H\}$ NMR spectroscopy was **1**. In contrast, methylation of **2s** either with 1 equiv. or with more than 2 equiv. of [Me_3O]BF_4 generates only [*mer-syn*-Ru(κ^2-OCO_2Me)(CO)(Cyttp)]BF_4 (**5s**(BF_4)) in high yield (Scheme 4). The different reactivities of **2a** and **2s** with >2 equiv. of [Me_3O]BF_4 may be attributed to **2a** being

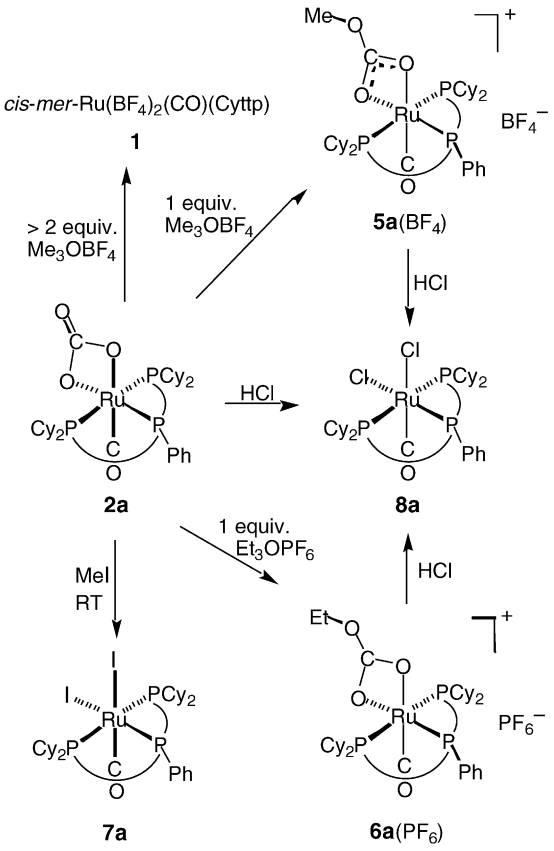

Scheme 3.

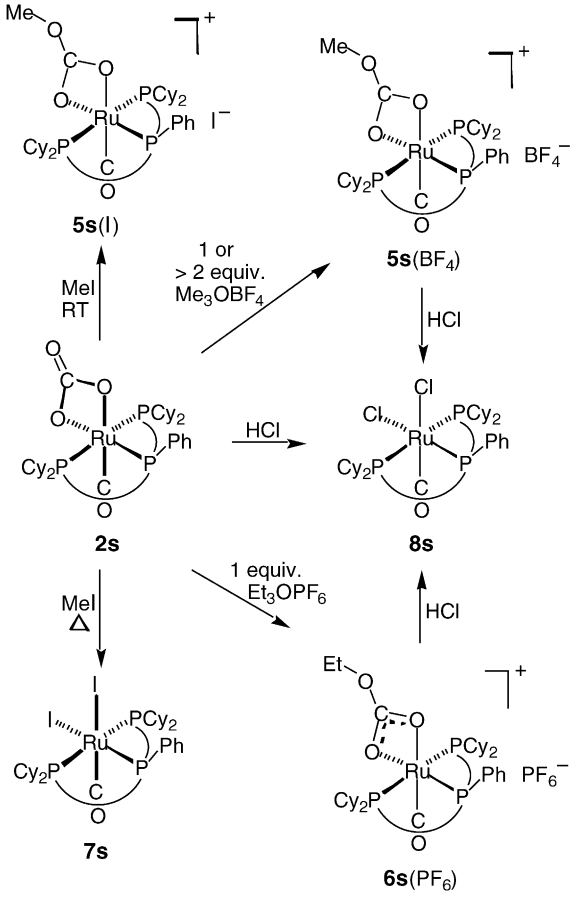

Scheme 4.

sterically less hindered than **2s** in the vicinity of Ru(κ^2-O_2CO) owing to the Cyttp Ph group's orientation away from this site. As a result, a second equivalent of $[Me_3O]BF_4$ methylates Ru-bonded oxygen in precursor **5a**(BF_4), thus leading to elimination of $(MeO)_2CO$ and replacement of the two oxygen donors with two BF_4^- ions at ruthenium. With the sterically more encumbered **2s**, methylation stops upon formation of **5s**(BF_4). These reactions represent, to our knowledge, the first example of different reactivity of *syn* and *anti* isomers of metal Cyttp complexes. Treatment of each **2a** and **2s** with 1 equiv. of $[Et_3O]PF_6$ resulted, as expected, in the formation of the ethylcarbonato complexes [*mer*-Ru(κ^2-O_2COEt)(CO)(Cyttp)]PF_6 as the *anti* (**6a**(PF_6)) and *syn* (**6s**(PF_6)) isomers, respectively. All of the complexes **5**(BF_4) and **6**(PF_6) were isolated as pure isomers, and no *syn*-to-*anti* or *anti*-to-*syn* conversion was observed. The structure of **5s**(BF_4) was determined by X-ray crystallographic techniques; the other *syn* and *anti* assignments are based on the (safe) assumption that the stereochemistry of the Cyttp Ph group is the same as in the precursor carbonato complex **2**. All assignments are supported by the NMR spectroscopic generalizations presented in Section 3.2.

Complex **2a** reacts slowly with an excess of MeI in benzene at room temperature to yield *cis-mer-anti*-RuI_2(CO)(Cyttp) (**7a**), previously prepared from *cis-mer*-Ru$(OSO_2CF_3)_2$(CO)(Cyttp) and NaI [10] (Scheme 3). When the reaction with MeI was carried out in C_6D_6 solution, a long-lived intermediate was detected by ^1H and $^{31}P\{^1H\}$ NMR spectroscopy which showed presence of *mer*-Cyttp and an OMe group. This intermediate may be a *mer*-RuI(OCO_2Me)(CO)(Cyttp) containing κ^1-methylcarbonato ligand; it is probably formed by alkylation of κ^2-carbonate in **2a** by Me^+ and substitution of one ligated oxygen by I^-. Further reaction with another molecule of MeI would give **7a** and $(MeO)_2CO$ (not identified).

Heating a solution of **2s** and an excess of MeI in THF at reflux temperature afforded *cis-mer-syn*-RuI_2(CO)(Cyttp) (**7s**) (Scheme 4). In contrast, by running the reaction at room temperature for 16 h, **5s**(I) was obtained. Possible conversion of **5s**(I) to **7s** with MeI under more forcing conditions was not investigated.

Reaction of **2s** with an excess of concentrated aqueous HCl in CH_2Cl_2 rapidly produced the dichloride *cis-mer-syn*-$RuCl_2$(CO)(Cyttp) (**8s**). This previously unreported isomer

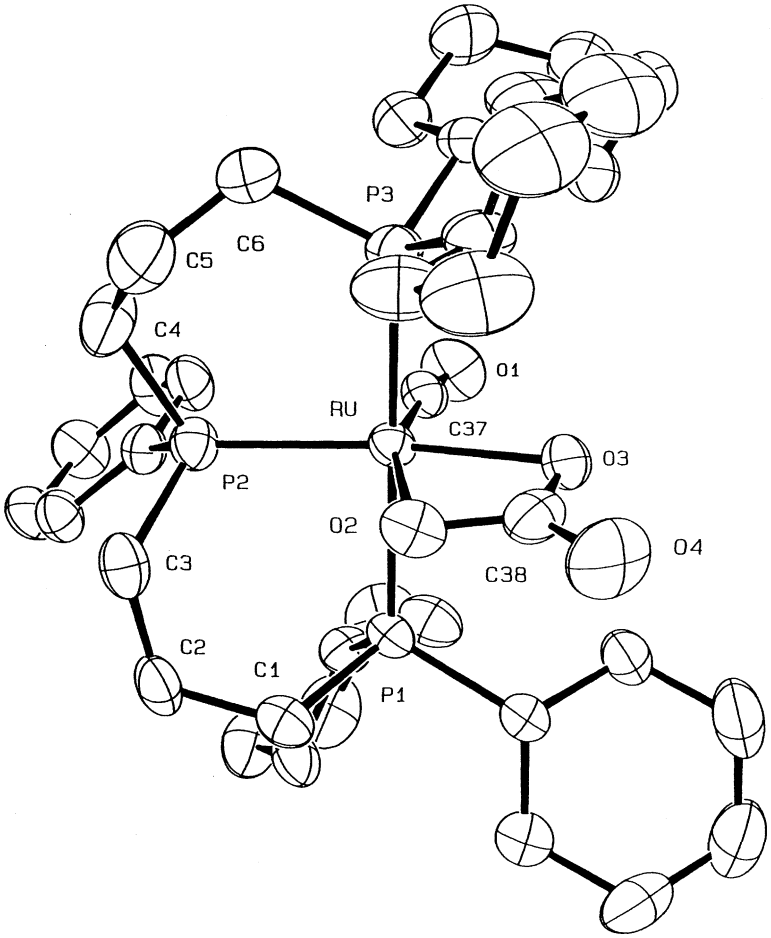

Fig. 1. Molecular structure of **2a**. Non-hydrogen atoms are represented by 50% probability ellipsoids. The hydrogen atoms are omitted for clarity.

of **2** was also prepared by a similar treatment of the alkylcarbonate **5s**(BF_4) or **6s**(PF_6) with HCl. The known *anti* isomer of **8**, *cis-mer-anti*-$RuCl_2$(CO)(Cyttp) (**8a**), resulted when each of the carbonato complex **2a**, carboxylato complexes **3a**(BF_4) and **4a**(BF_4), or alkylcarbonato complexes **5a**(BF_4) and **6a**(PF_6) was treated similarly with hydrochloric acid. All of the dihalide complexes *cis-mer*-RuX_2(CO)(Cyttp) (X = Cl or I) are stable with respect to *syn–anti* isomerization.

3.2. Characterization of products

All new complexes were characterized by a combination of IR and NMR (^{1}H, ^{31}P$\{^1$H$\}$, and ^{13}C$\{^1$H$\}$) spectroscopy, FAB mass spectrometry, and elemental analysis. The structures of **2a** (as **2a**·CH_2Cl_2·$2H_2O$), **2s** (as **2s**·(3/4)MeC(O)Me·$2H_2O$), and **5s** (as **5s**(BF_4)·C_6H_6)) were elucidated by X-ray diffraction techniques.

The meridional orientation of the Cyttp ligand in all complexes is indicated by both the A_2X pattern in the ^{31}P$\{^1$H$\}$ NMR spectra [6,7,9,10] and the ^{13}C$\{^1$H$\}$ NMR resonances for the CH cyclohexyl carbon atoms, which appear as virtual triplets [29] at δ 42.1–33.1 ppm (J_{PwC} = 10–12 Hz) and 38.6–32.5 ppm (J_{PwC} = 9–11 Hz). The lone CO ligand is in all cases *cis* to the three P donors, as shown by either equal or similar coupling of the carbonyl carbon to the central (P_c) and the wing (P_w) phosphorus atoms ($^2J_{PcC} \sim {}^2J_{PwC}$). These assignments leave the remaining two *cis*-octahedral positions for occupancy by two halides or a bidentate carbonato, carboxylato, or alkylcarbonato ligand. The IR spectra of **2a** and **2s** [25] exhibit $\nu(O_2CO)$ absorptions expected for bidentate carbonate [30], and those of **3a**(BF_4) and **4a**(BF_4) and of **5a**(BF_4), **5s**(BF_4), **6a**(PF_6), and **6s**(PF_6) show related absorptions of bidentate carboxylate and alkylcarbonate, respectively [31]. The IR spectra of the aforementioned complexes also display a strong (CO) absorption, which occurs, as expected, at 1918–1915 cm^{-1} for the electrically neutral metal carbonates **2a** and **2s** [25] and at 1960–1935 cm^{-1} for the cationic metal carboxylates and alkylcarbonates. The presence of these ligands is also reflected by the appearance in the ^{13}C$\{^1$H$\}$ NMR spectra of the appropriate signal at δ 166 ppm for **2**, 187 ppm for **3** and **4**, and 161 ppm for **5** and **6**.

The crystallographically determined structures of **2a**, **2s**, and **5s** are presented with ORTEP drawings in Figs. 1–3, respectively. Selected bond distances and angles are given in Table 2.

The three structures show the *anti* orientation of the Ph group in **2a** and the *syn* orientation in **2s** and **5s**, but reveal no unusual features. All bond distances and angles fall within

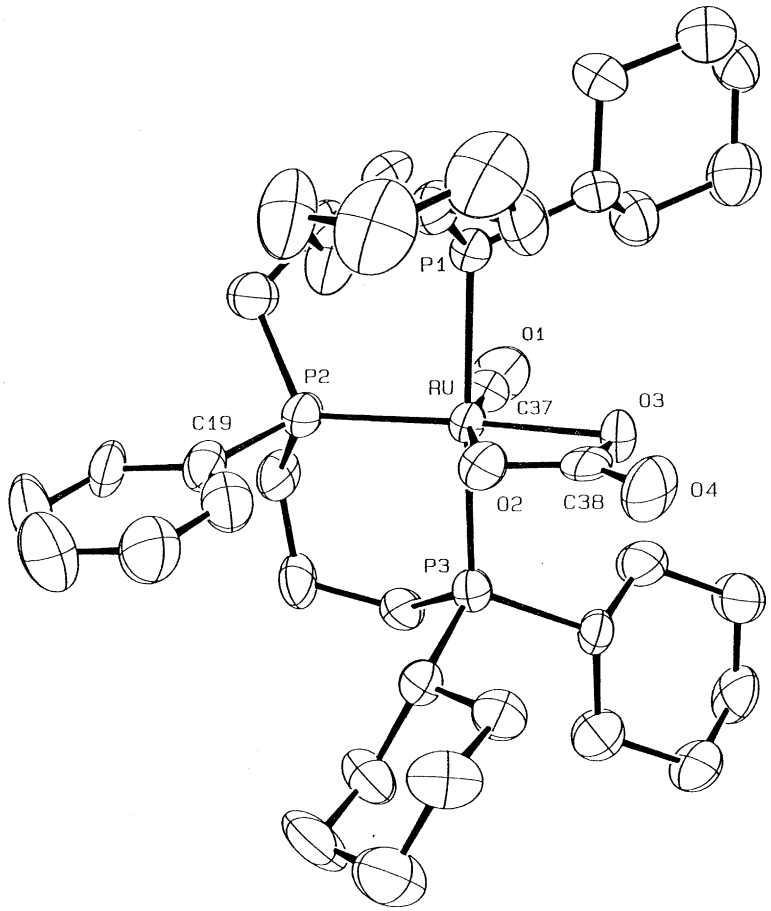

Fig. 2. Molecular structure of **2s**. Non-hydrogen atoms are represented by 50% probability ellipsoids. The hydrogen atoms are omitted for clarity.

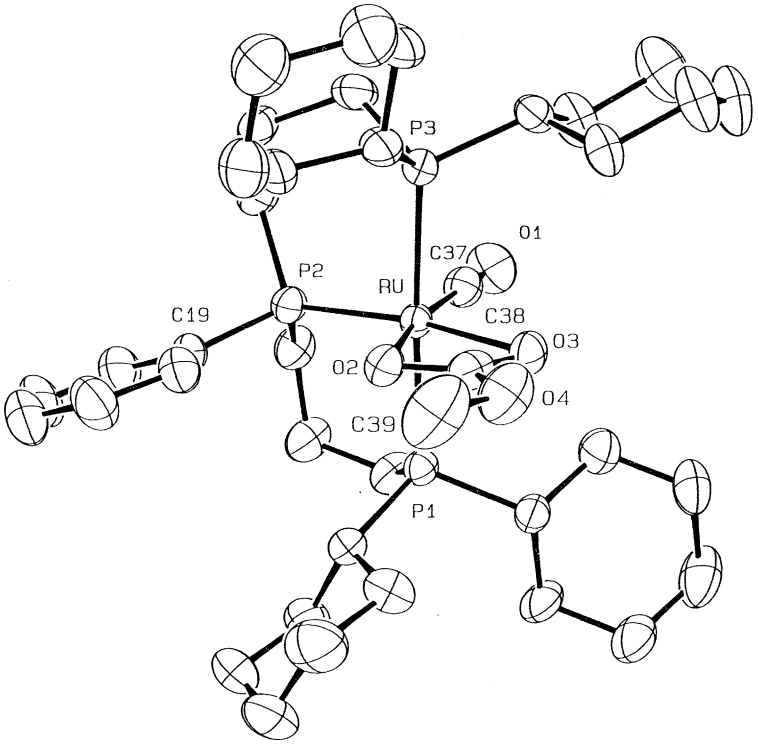

Fig. 3. Molecular structure of **5s**. Non-hydrogen atoms are represented by 50% probability ellipsoids. The hydrogen atoms are omitted for clarity.

normal ranges for comparable complexes. The Ru–O bond distances vary from 2.119(4) to 2.143(4) Å for the carbonates **2a** and **2s**, being similar to the distance 2.087(5) Å found in Ru(κ^2-O_2CO)(bipy)$_2$ [32]. For **5s**, the Ru–O bond distances of 2.185(4) and 2.205(4) Å are consistent with those found in related complexes [33–35]. The carbon–oxygen bond lengths of **2a** and **2s** (cf. Table 2) are close to those found in other carbonato complexes [36,37] and indicate considerable localization of these bonds, viz., Ru(–O)$_2$C=O. The corresponding bonds of **5s** – O(2)–C(38) 1.261(6), O(3)–C(38) 1.251(7), O(4)–C(38) 1.335(6) Å – suggest a delocalized ligand representation, Ru(–O)$_2$C–OMe. The C–O bond length of 1.335(6) Å compares well with that reported for organic carbonates (1.34 Å av. [38]). Concerning Ru–Cyttp bonding, the shorter Ru–P(2) bond as compared to Ru–P(1) and Ru–P(3) in each of **2a**, **2s**, and **5s** is typical of meridional Cyttp complexes with weakly *trans*-labilizing ligands opposite to P$_c$ [3,10].

Apart from orientation of the Ph group, the most important difference in structure between the *anti* isomer **2a** and the *syn* complexes **2s** and **5s** is the magnitude of the angle P(2)–Ru–C(37). This angle is substantially larger for **2a** (96.3(2)°) than for **2s** (84.4(4)°) or **5s** (84.2(2)°). Significantly, the angle P(2)–Ru–O(2) is larger for **2s** (109.0(2)°) and **5s** (107.8(1)°) than for **2a** (101.9(1)°); however, the difference is not as pronounced as that for the angle P(2)–Ru–C(37). These structural results may be rationalized by a greater steric repulsion between the phenyl group on P(2) and the carbonate oxygen O(2) in **2s** and **5s** than between the phenyl group on P(2) and CO in **2a**. Interestingly, the structurally characterized *syn* and *anti* isomers of *mer*-RuCl(η^3-PhCH=C–C≡CPh)(Cyttp) show a pronounced difference in the angle P$_c$–Ru–Cl, which is greater for the former, and a less pronounced difference in the angle P$_c$–Ru–(vinyl C), which is greater for the latter [8].

Complex **2a** also differs from **2s** and **5s** with respect to displacement of the Ru center from the plane of three P donor atoms. Whereas Ru is nearly coplanar with the P atoms in **2s** and **5s** (a displacement of 0.0321 and 0.0028 Å, respectively, toward the CO), it is substantially out of that plane in **2a** (0.1488 Å toward the CO). Furthermore, the position of Ru with reference to the P$_3$ plane is reflected in the magnitude of the P(1)–P(2)–P(3) bond angle, which is 172.85(6)° for **2a**, but closer to 180°, viz., 176.6(1) and 176.11(5)°, for **2s** and **5s**, respectively.

The aforementioned structural differences between the *syn* and the *anti* complexes affect certain aspects of their $^{13}C\{^1H\}$ and $^{31}P\{^1H\}$ NMR spectra. Interestingly, resultant differences in NMR spectroscopic properties are observed not only for **2a**, **2s**, and **5s**, but also for the other *syn* and *anti* complexes of the type [*mer*-Ru(κ^2-O_2CX)(CO)(Cyttp)]$^+$ (**3**–**6**) and *cis*-*mer*-RuX$_2$(CO)(Cyttp) (**7**, **8**) obtained in this study. Such general behavior would seem to indicate that the *syn*–*anti* differences in structure extend to this whole group of complexes.

The values of $^2J_{PcC}$ for the ^{13}C resonance of CO are invariably larger for the *syn* than for the corresponding *anti* isomers (Δ = 4–9 Hz). This appears to be a consequence of the relative

Table 2
Selected bond distances (Å) and bond angles (°) of **2a**·CH_2Cl_2·$2H_2O$, **2s**·(3/4)MeC(O)Me·$2H_2O$, and **5s**(BF_4)·C_6H_6

	2a	2s	5s
Ru—P(1)	2.400(2)	2.3402(3)	2.397(1)
Ru—P(2)	2.314(2)	2.303(3)	2.279(1)
Ru—P(3)	2.444(2)	2.404(3)	2.439(2)
Ru—O(2)	2.121(4)	2.126(7)	2.185(4)
Ru—O(3)	2.119(4)	2.143(6)	2.205(3)
Ru—C(37)	1.821(6)	1.809(14)	1.824(6)
O(1)—C(37)	1.160(7)	1.170(13)	1.151(6)
O(2)—C(38)	1.320(7)	1.323(12)	1.261(6)
O(3)—C(38)	1.296(7)	1.299(13)	1.251(7)
O(4)—C(38)	1.236(7)	1.263(12)	1.335(6)
O(4)—C(39)			1.430(8)
P(1)—Ru—P(2)	87.69(6)	92.6(1)	88.77(5)
P(1)—Ru—P(3)	172.85(6)	176.6(1)	176.11(6)
P(1)—Ru—O(2)	82.6(1)	88.5(2)	90.4(1)
P(1)—Ru—O(3)	92.2(1)	87.4(2)	88.1(1)
P(1)—Ru—C(37)	91.9(2)	92.3(3)	90.0(2)
P(2)—Ru—P(3)	93.05(6)	90.5(1)	95.12(5)
P(2)—Ru—O(2)	101.9(1)	109.0(2)	107.8(1)
P(2)—Ru—O(3)	163.6(1)	171.3(2)	167.2(1)
P(2)—Ru—C(37)	96.3(2)	84.9(4)	84.2(2)
P(3)—Ru—O(2)	90.3(1)	89.0(2)	88.3(1)
P(3)—Ru—O(3)	85.1(1)	89.4(2)	88.1(1)
P(3)—Ru—C(37)	95.1(2)	89.6(3)	90.5(2)
O(2)—Ru—O(3)	61.9(2)	62.3(2)	59.8(1)
O(2)—Ru—C(37)	160.7(2)	166.0(4)	168.0(2)
O(3)—Ru—C(38)	100.0(2)	103.8(4)	108.2(2)
Ru—O(2)—C(38)	92.1(4)	91.5(7)	89.7(3)
Ru—O(3)—C(38)	92.9(3)	91.4(6)	89.1(3)
O(2)—C(38)—O(3)	113.0(5)	115(5)	121.3(5)
O(2)—C(38)—O(4)	122.9(7)	122(1)	122.3(6)
O(3)—C(38)—O(4)	124.1(6)	123(1)	116.4(5)
Ru—C(37)—O(1)	172.9(5)	178(1)	178.7(5)
Ru—P(2)—C(19)	119.9(2)	118.7(4)	116.8(2)
C(38)—O(4)—C(39)			116.6(5)

size of the angle P_c–Ru–C(of CO). Carty and coworkers have shown that $^2J_{PcC}$ depends on the P–M–C bond angle, increasing as the angle progressively decreases below 110° [39]. In the $^{31}P\{^1H\}$ NMR spectra, the resonance of P_c is downfield from the resonance of P_w in each of the complexes **2**–**8** (Δ = 4–24 ppm, and generally 16–24 ppm). This relationship results from a weak *trans*-labilizing ligand being opposite to P_c [3]. In addition, the resonance of P_c for each *anti* isomer is downfield with respect to the corresponding resonance for the *syn* isomer (generally by 7–9 ppm), and $^2J_{PcPw}$ is slightly larger for the *anti* isomer (Δ = 1.3–3.3 Hz). These trends are a direct consequence of the displacement of Ru from the P_3 plane. For example, a larger displacement of the Ru atom for **2a** than for **2s** is expected to result in a poorer overlap of the phosphorus and metal orbitals, thus leading to a greater deshielding of P_c in the former compared to the latter isomer.

4. Discussion and conclusion

The impetus for this research was to gain further insight into *syn–anti* configurational behavior of six-coordinate ruthenium(II) Cyttp complexes in isomerization and ligand substitution reactions. Previous studies revealed that some complexes display high configurational stability while other complexes show propensity to undergo *syn–anti* isomerization [7,8,10,20].

We find in this investigation that octahedral ruthenium(II) complexes of the type [*mer*-Ru(κ^2-O_2CX)(CO)(Cyttp)]^n (n = 0, **2**; n = +1, **3**–**6**) and *cis-mer*-RuX_2(CO)(Cyttp) (**7**, **8**), all containing ligands that do not readily dissociate, display high stability toward *syn*-to-*anti* and/or *anti*-to-*syn* isomerization. This behavior may be contrasted with that reported for **1** and *cis-mer*-Ru$(OSO_2CF_3)_2$(CO)(Cyttp) with weakly coordinating anionic ligands, for which *syn–anti* isomerization has been implicated by solution NMR spectra [10]. Further examples of observed isomerization include *syn*-to-*anti* conversions of *cis-mer*-RuH_2(P(OPh)$_3$)(Cyttp) [20] and *mer*-RuCl(η^3-PhCH=C–C≡CPh)(Cyttp) [7,8]. The former has been attributed to steric factors (bulky P(OPh)$_3$ ligand *syn* to the Ph group of Cyttp in the reactant), whereas the latter is likely driven by a stronger Ru–(η^2-C≡C) interaction in the *anti* product than in the *syn* reactant, as inferred from crystallographic data [8]. Thus, it appears that formation of a five-coordinate intermediate in these reactions triggers *syn–anti* isomerization.

Ligand substitution reactions of ruthenium(II) Cyttp complexes support the foregoing generalization. Reactions of freshly prepared solutions (to forestall isomerization) of the *anti* isomer of **1** or of *cis-mer*-Ru$(OSO_2CF_3)_2$(CO)(Cyttp) with various ligands, for example, CO_3^{2-}, RCO_2^-, Cl^-, I^- [10], and H^- [10], lead to retention of the orientation of the Ph group of Cyttp in the products. The same stereochemical result was obtained when **2a** and **2s** reacted with HCl to give **8a** and **8s**, respectively. Likewise, replacement of η^2-H_2 in *cis-mer*-RuH_2(η^2-H_2)(Cyttp) with CO, N_2, or $PhCH_2NC$ proceeds to a single isomer of each product [20]. In contrast, corresponding reaction with P(OMe)$_3$ affords a mixture of the *syn* and *anti* isomers of *syn-mer*-RuH_2(P(OMe)$_3$)(Cyttp), probably owing to *syn*-to-*anti* conversion for steric reasons of the initially formed product [20], as for the analogous P(OPh)$_3$ complex (vide supra).

Dissociatively stable six-coordinate ruthenium(II) Cyttp complexes do not undergo *syn–anti* isomerization, since no low energy intramolecular process exists that would effect such a transformation. However, for five-coordinate trigonal bipyramidal complexes, *syn–anti* isomerization can take place by an exchange process that interconverts two of the three equatorial as well as the two axial ligands. This mechanism will be considered in a subsequent publication dealing with additional chemistry of ruthenium Cyttp complexes [40].

Acknowledgements

This study was supported in part by the National Science Foundation and The Ohio State University.

References

[1] F.A. Cotton, B. Hong, Prog. Inorg. Chem. 40 (1992) 179.
[2] D.W. Allen, in: D.W. Allen, J.C. Tebby (senior reporters), Organophosphorus Chemistry, RSC Specialist Periodical Report, vol. 32, Cambridge, UK, 2002, p. 1 and previous volumes in this series.
[3] (a) R. Mason, D.W. Meek, Angew. Chem., Int. Ed. Engl. 17 (1978) 183;
(b) D.W. Meek, T.J. Mazanec, Acc. Chem. Res. 14 (1981) 266.
[4] R.B. King, in: E.C. Alyea, D.W. Meek (Eds.), Catalytic Aspects of Metal Phosphine Complexes, Advances in Chemistry Series, vol. 196, American Chemical Society, Washington, DC, 1982, p. 313.
[5] R. Uriarte, T.J. Mazanec, K.D. Tau, D.W. Meek, Inorg. Chem. 19 (1980) 79.
[6] G. Jia, D.W. Meek, J.C. Gallucci, Organometallics 9 (1990) 2549.
[7] G. Jia, D.W. Meek, Organometallics 10 (1991) 1444.
[8] G. Jia, J.C. Gallucci, A.L. Rheingold, B.S. Haggerty, D.W. Meek, Organometallics 10 (1991) 3459.
[9] G. Jia, D.W. Meek, Inorg. Chem. 30 (1991) 1953.
[10] P.W. Blosser, J.C. Gallucci, A. Wojcicki, Inorg. Chem. 31 (1992) 2376.
[11] Y. Kim, D.E. Rende, J.C. Gallucci, A. Wojcicki, Inorg. Chim. Acta 352 (2003) 171.
[12] Y. Kim, D.E. Rende, J.C. Gallucci, A. Wojcicki, J. Organomet. Chem. 682 (2003) 85.
[13] R.S. Cahn, C. Ingold, V. Prelog, Angew. Chem., Int. Ed. Engl. 5 (1966) 385.
[14] J.B. Letts, T.J. Mazanec, D.W. Meek, J. Am. Chem. Soc. 104 (1982) 3898.
[15] L.M. Koczon, R.C. Tisdale, K. Gebreyes, T.A. George, L. Ma, S.N. Shaikh, J. Zubieta, Polyhedron 9 (1990) 545.
[16] T. Zhu, W.G. Jackson, Inorg. Chim. Acta 343 (2003) 147.
[17] T. Zhu, W.G. Jackson, Inorg. Chem. 42 (2003) 88.
[18] E. Arpec, L. Dahlenberg, Z. Naturforsch. 36 (1981) 672.
[19] C. Yang, S.M. Socol, D.J. Kountz, D.W. Meek, Inorg. Chim. Acta 114 (1986) 119.
[20] G. Jia, D.W. Meek, J.C. Gallucci, Inorg. Chem. 30 (1991) 403.
[21] D.F. Shriver, M.A. Drezdzon, The Manipulation of Air-sensitive Compounds, 2nd ed., Wiley, New York, 1986.
[22] D.D. Perrin, W.L.F. Armarego, D.R. Perrin, Purification of Laboratory Chemicals, Pergamon Press, Oxford, 1991.
[23] R.R. Willis, M. Calligaris, P. Faleschini, J.C. Gallucci, A. Wojcicki, J. Organomet. Chem. 193/194 (2000) 465.
[24] R.T. Dunsizer, V.M. Marsico, V. Plantevin, A. Wojcicki, Inorg. Chim. Acta 342 (2003) 279.
[25] J.B. Letts, T.J. Mazanec, D.W. Meek, Organometallics 2 (1983) 695.
[26] TEXSAN, Single Crystal Structure Analysis Software, Version 5.0, Molecular Structure Corp., The Woodlands, TX, 1989.
[27] (a) International Tables for X-ray Crystallography, vol. IV, Kynoch Press, Birmingham, UK, 1974, pp. 71 and 148;
(b) R.F. Stewart, E.R. Davidson, W.T. Simpson, J. Chem. Phys. 42 (1965) 3175.
[28] A.C.T. North, D.C. Phillips, F.S. Mathews, Acta Crystallogr. A 24 (1968) 351.
[29] L.M. Wilkes, J.H. Nelson, L.B. McCusker, K. Seff, F. Mathey, Inorg. Chem. 22 (1983) 2476.
[30] K. Nakamoto, Infrared and Raman Spectra of Inorganic and Coordination Compounds, 3rd ed., Wiley, New York, 1978, pp. 243–245.
[31] K. Nakamoto, Infrared and Raman Spectra of Inorganic and Coordination Compounds, 3rd ed., Wiley, New York, 1978, pp. 232–233.
[32] T. Kimlera, T. Sakurai, M. Shima, T. Nagai, K. Mizumachi, Acta Crystallogr. Sect. B 38 (1982) 112.
[33] (a) T.V. Ashworth, M. Nolte, E. Singleton, J. Organomet. Chem. 121 (1976) C57;
(b) T.V. Ashworth, M. Nolte, E. Singleton, J. Chem. Soc., Dalton Trans. (1976) 2184.
[34] E.B. Boyar, A. Harding, S.D. Robinson, C.P. Brock, J. Chem. Soc., Dalton Trans. (1986) 1771.
[35] R.A. Sanchez-Delgado, U. Thewalt, N. Valencia, A. Andriollo, R.-L. Marquez-Silvin, J. Puga, H. Schollhorn, H.-P. Klein, B. Fontal, Inorg. Chem. 25 (1986) 1097.
[36] M.C. Favas, D.L. Keport, J.M. Patrick, A.H. White, J. Chem. Soc., Dalton Trans. (1983) 571.
[37] M.D. Curtis, K.R. Han, Inorg. Chem. 24 (1985) 378.
[38] (a) F. Cser, Acta Chim. Acta Sci. Hung. 80 (1974) 49;
(b) A.M. Sorensen, Acta Chem. Scand. 25 (1971) 169.
[39] L.H. Randall, A.A. Cherkas, A.J. Carty, Organometallics 8 (1989) 568.
[40] P.W. Blosser, A. Wojcicki, in preparation.